Bulgarian Journal of Agricultural Science, 31 (No 5) 2025, 895–904

Evaluation of the antibacterial effect of silver nanoparticles synthesized from the liquid cultivation of *Trichoderma* spp. Isolated from farming soil

Do Tan Khang, Tran Trung Vinh, Tran Thi Cam Lien, Tran Ngoc Quy and Nguyen Pham Anh Thi*

Can Tho University, Department of Molecular Biology, Institute of Food and Biotechnology, Can Tho City, Vietnam
**Corresponding author:* npathi@ctu.edu.vn

Abstract

Khang, D. T., Vinh, T. T., Tran, L. Th. C., Tran, N. Q. & Nguyen, Ph. A. Th. (2025). Evaluation of the antibacterial effect of silver nanoparticles synthesized from the liquid cultivation of *Trichoderma* spp. Isolated from farming soil. *Bulg. J. Agric. Sci., 31*(5), 895–904

Silver nanoparticles (AgNPs) synthesized by the biological method are an inexpensive and straightforward approach that offers several advantages over physicochemical processes, particularly in terms of environmental friendliness. In this study, AgNPs were synthesized using the fungus *Trichoderma virens* (*T. virens*) isolated from farming soil. The fungal filtrate containing a silver ion-reducing agent reacted with a silver nitrate solution, resulting in the formation of AgNPs. The synthesis of nano silver is optimized for various factors, including $AgNO_3$ concentration, the ratio of $AgNO_3$ solution to fungal filtrate, pH level, and synthesis time. Optical properties, shape, and structure of the synthesized AgNPs were characterized using visual analysis, ultraviolet-visible (UV-Vis) spectroscopy, and scanning electron microscopy (SEM). The antibacterial activity of synthesized AgNPs against *Escherichia coli* (*E. coli*), *Staphylococcus aureus* (*S. aureus*), and *Propionibacterium acnes* (*P. acnes*) at concentrations of 100%, 75%, 50%, and 25% was investigated using the agar well diffusion method. The particle sizes of the synthesized AgNPs ranged from 70 to 100 nm. For the synthesis conditions, the optimized $AgNO_3$ concentration, ratio $V_{AgNO3}/V_{fungal\ filtrate}$, pH, and reaction time were 1.6 mM, 27.4%, 7.9, and 71.2 h, respectively. The AgNPs with a 100% concentration showed the highest antibacterial effect against *Escherichia coli*, *Staphylococcus aureus*, and *Propionibacterium acnes,* with the diameter of the inhibited zone being approximately 11.93 ± 0.24 mm, 8.83 ± 0.18 mm, and 6.67 ± 0.29 mm, respectively.

Keywords: antibacterial; *Trichoderma fungus*; nano silver; *Propionibacterium acnes*; *Staphylococcus aureus*

Introduction

Silver metal (Ag) has been used as a precious metal with outstanding antibacterial activity for thousands of years. However, until now, silver has not been widely used in everyday life due to its high cost. In recent years, nanotechnology has undergone significant development and application in various scientific fields, including biomedicine, optics, information technology, catalysis, cosmetics, and apparel. Nanotechnology can be considered a leap and a breakthrough in science, engineering, and technology, in which nanosilver technology has garnered much attention from researchers. Silver nanomaterials combine the superior properties of nanomaterials with the characteristic properties of silver metal; thus, they have a wide range of potential applications, particularly in inhibiting a broad spectrum of bacterial strains (Loo et al., 2018). Many recent medical studies have shown that nano silver can inhibit over 650 different strains of bacteria, especially intestinal bacteria that can easily affect human health, such as *E. coli*. The antibacterial mechanism of nano silver has been proven not to affect animal cells; thus, nano silver is considered a safe antibiotic for humans. In addition, many public health organizations warn that the antibiotic-resistant issue will worsen because

there are not enough new antibiotics in development to combat antibiotic-resistant bacteria. Meanwhile, AgNPs with significant antibiotic activity offer a new powerful tool for humanity to combat antibiotic-resistant bacteria, as there is no evidence indicating that bacteria possess a mechanism to resist AgNPs.

However, the challenging issues in current nanotechnology include the development of reliable experimental techniques for synthesizing nanoparticles of different compositions and sizes, along with high monodispersity. The use of microorganisms for the deliberate synthesis of nanoparticles is a relatively new and exciting area of research with considerable potential for further development.

Many research works have successfully synthesized nano silver using various approaches, including physics and chemistry. Physical methods often have low efficiency, while chemical methods require high costs, modern equipment, and extreme conditions, including high pressure and temperature, as well as the use of potentially harmful chemicals. Detoxification has the potential to cause environmental pollution, which can impact both the ecosystem and human health (Wang et al., 2007). The recent trend of synthesizing AgNPs through a biological route, using reducing agents obtained from cultures, and extracting them from biological agents has become an alternative method, overcoming the limitations of processes synthesized by conventional physical and chemical methods. According to Berdy (2005), filamentous fungi have greater potential to synthesize AgNPs than other microorganisms because they can synthesize over 6,400 biological compounds, including proteins, enzymes, and other secondary metabolites. There have been numerous studies conducted by various authors worldwide on the application of fungi, particularly the genus *Trichoderma* sp., in the synthesis of AgNPs, as it offers several advantages over other methods. Thanks to the excellent properties of the genus *Trichoderma* sp., particularly its tolerance to high concentrations of heavy metals, ability to absorb and metabolize metals, and ease of growing biomass on a large scale. Mycosynthesis of AgNPs offers several advantages, including simplicity, cost savings, and environmental friendliness, while still ensuring the biochemical and physical activity and durability of AgNPs.

Based on the above issues, the topic "Evaluation of the antibacterial effect of silver nanoparticles synthesized from liquid cultivation of *Trichoderma* spp. isolated from farming soil" was investigated. The objectives of this topic are the isolation of *Trichoderma* fungus from agricultural soil samples, the synthesis of AgNPs from *Trichoderma* fungal filtrate, and the investigation of the antibacterial activity of the synthesized AgNPs.

Materials and Methods

Samples and culture media

Samples of soil were collected from a farm in Ninh Kieu District, Can Tho City. All experiments were conducted from August 2022 to March 2023. Culture media consist of Luria-Bertani agar (LB), Luria-Bertani broth (LB broth), potato dextrose agar (PDA), Trichoderma selective medium (TSM), Czapek-Dox broth (CDB), and tryptone soy agar (TSA).

Bacterial strains *E. coli* (ATCC® 25922TM) and *S. aureus* (ATCC® 25923TM) were provided by the Molecular Biotechnology Laboratory, Biotechnology R&D Institute, Can Tho University. *Propionibacterium acnes* PO was isolated and identified by Bui et al. (2021) in their research.

Isolation and culture of Trichoderma spp.

Soil samples for the isolation of *Trichoderma* spp. were obtained using the method described by Elad et al. (1982). A sterile knife was used to remove the topsoil gently, and each sample was taken randomly at a depth of 20 cm (300 g/g/sample). After that, soil samples were placed in plastic bags, labeled, and preserved in the laboratory.

The homogenous sample was mixed well and spread on a dry tray (wiped with 70% alcohol and heated over a flame). After removing plant roots and undesirable objects, 10 g of soil sample was placed in a conical flask containing 90 mL of sterile distilled water. Then, the sample was shaken for 5 to 10 min so that the microorganisms in the mixture were evenly distributed.

A volume of 1 mL of the initial suspension was loaded into a test tube containing 9 mL of sterile distilled water (avoiding touching the sterile micropipette with the diluent). The mixture was thoroughly mixed on a Vortex to obtain a sample dilution of 10^{-2}. Then, each suspension was serially diluted up to 10^{-5}.

On two Petri dishes containing Trichoderma-specific medium (TSM), 0.1 mL of the initial suspension was placed on each dish. The procedure was repeated with further dilutions.

Using a sterile swab, evenly spread the suspension over the surface of the agar plates. The Petri dishes were left at room temperature for approximately 15 min, until all liquids had dried completely, followed by incubation at 37°C for 2–3 days. After 2–3 days, the fungal colonies on the agar surface were selected based on their typical characteristics of the genus *Trichoderma*. The selected colonies were then transferred to TSM medium and incubated at room temperature for 2–3 days.

For pure isolation, the colonies were transferred from TSM medium to Potato Dextrose Agar (PDA) medium and

cultured at room temperature for 24 h. After 24 h, agar containing mycelium was cut and subcultured in PDA medium. Sample dishes were incubated at 37°C for 2–3 days, and then the colony characterization was observed in comparison to previously isolated colonies.

The pure fungal strain was maintained on PDA slant agar and incubated at room temperature for 2–3 days. It was then preserved in the refrigerator and reinoculated after 30 days.

Preparation of a specimen for observation of mycelium: an agar piece from selected colonies was cut (size 0.5 × 0.5 cm) and placed on a glass slide. A volume of 30 µL of methylene blue dye was loaded into the mycelium. The surface of the glass slide was covered by a lamella (avoiding air bubbles). Then, microscopic examination of slides and characterization of mycelium and fungal spores were performed.

Identification of Trichoderma fungus strains by molecular biology method.

Rapid DNA extraction consists of six steps. Step 1: Use a sterile inoculation needle to take the mycelium into a 2.2 mL tube. Add one iron bead soaked with 96% alcohol in the tube. Add 50 µL of Lysis Buffer (LB) and homogenize with a mixer mill for three cycles of 10 s at a frequency of 30 times/s. Step 2: Add 950 µL of Lysis Buffer (LB) to the tube, shake vigorously several times, and then incubate at room temperature for 10 min. Step 3: Centrifuge at 12,000 rpm for 10 min at room temperature. Then, pipette 500 µL of the supernatant into a 1.5 mL tube containing 1 mL of absolute ethanol. Gently invert the tube and incubate the sample for 30 min at room temperature. Step 4: Centrifuge at 12,000 rpm for 10 minutes at room temperature. Discard the alcohol and retain the precipitate. Step 5: Add 700 µL of 70% ethanol and centrifuge at 12,000 rpm for 10 min (repeat this step twice). Step 6: carefully discard the ethanol, retain the precipitate, and dry the DNA using a vacuum centrifuge (60°C for 10 min). Add 100 µl 0.1X TE to resuspend the DNA and store at −20°C.

PCR reaction: The rDNA−ITS gene region was selected for amplification with the primer pairs ITS1 (5' TCC GTA GGT GAA CCT GCG G 3') and ITS4 (5' TCC TCC GCT TAT TGA TAT GC 3') (White et al, 1990). The PCR reaction was performed with a total volume of 25 µL, consisting of 12 µL of H_2O, 10 µL of 2X master mix, 0.5 µL of each forward primer and reverse primer (20 µM), and 2 µL of DNA with a concentration of 50 ng/µL. The thermal cycling profile of the PCR reaction is shown in Table 1.

Evaluation of PCR reaction by electrophoresis: The PCR products were electrophoresed on a 2% agarose gel. A volume of 15 mL of TBE 1X was dissolved with 2% agarose in the microwave. The agarose was then poured into the tray. A drop of 2 µL Loading buffer was divided evenly on parafilm paper. Then, 5 µL of the sample was loaded into the Loading buffer drop and mixed, followed by addition to the well on the agarose gel. The tray was placed in the electrophoresis bath and covered with 1X TBE. Electrophoresis was conducted at 50 volts for 30 min. Pictures of the gel were obtained using a Bio-Rad Gel Doc 2000. PCR products were sequenced at the Next Gen company in Ho Chi Minh City. The sequenced results were then compared with the data on GenBank NCBI using the BLAST tool to determine the similarity of this gene region sequence with that of published fungal strains.

Table 1. Thermocycling profile

Phases	Temperature, °C	Time	No. of Cycle
Initial denaturation	95	5 min	1
Denaturation	95	40 s	30
Annealing	57	30 s	
Extension	72	1.5 min	
Final extension	72	7 min	1
Hold	4	+∞	1

Process of synthesizing and investigating AgNPs

Collecting biomass and filtrate of *Trichoderma* fungus: pure mycelium was cultured in a flask containing 200 mL of Czapek Dox broth and shaken in a shaking incubator at 150 rpm under 35 – 37°C for 2 – 3 days. Fungal biomass was collected by filtration and washing with distilled water through Whatman filter paper (10 mm diameter) to remove the medium and other impurities. The filtrated fungi were continued to grow the fungal biomass in a conical flask containing 200 mL of sterile distilled water. The conical flask was then shaken in a shaking incubator at 150 rpm under 35–37°C for 2–3 days. Whatman filter paper (10 mm in diameter) was used to collect the filtrate and remove the fungal biomass.

Synthesized AgNPs: AgNPs were synthesized by mixing the obtained filtrate with one mM $AgNO_3$ solution at a ratio of 1:15 (v/v). The mixture was then incubated and shaken in the dark at 150 rpm and 35–37 °C for 24 h. The negative control contained distilled water instead of the $AgNO_3$ solution.

Rating criteria: the reduction of metal ions was monitored by observing the color change of the solution during the reaction and the UV-visible absorption spectrum.

Optimization of conditions for the biosynthesis of AgNPs

The experiment was arranged in a completely randomized design using *Trichoderma* filtrate, with four factors ($AgNO_3$ concentration, ratio of $AgNO_3$ solution to fungal filtrate (v/v), pH, and reaction time) and three replications in

a Central Composite Design (CCD) format, based on Design Expert 13.0 software. The ranges of values of four factors are shown in Table 2.

The procedure for optimal experiment: Biomass of *T. virens* was cultivated in 200 mL CDB medium (incubated at 150 rpm in the dark for 2–3 days at 35–37°C). Fungal biomass was harvested (sieving through a filter paper followed by washing with deionized water) and then cultured in 200 mL of sterile distilled water. The cell filtrate was collected and mixed with an $AgNO_3$ solution at the concentrations and ratios ($AgNO_3$ solution/fungal filtrate) shown in Table 2, along with the corresponding pH values. The investigation of AgNPs solutions synthesized over time was conducted by determining the AgNPs formation through the absorption maximum value at 420 nm (OD420 nm).

Table 2. The results of factors affecting the formation of AgNPs

Treatments	A	B	C	D	OD_420 nm
1	0.5	50	6	24	$0.067^{j} \pm 0.006$
2	1.25	27.5	7.5	48	$0.682^{a} \pm 0.017$
3	0.5	5	6	24	$0.014^{j} \pm 0.007$
4	1.25	27.5	9	48	$0.682^{a} \pm 0.017$
5	1.25	27.5	7.5	48	$0.682^{a} \pm 0.033$
6	0.5	5	9	72	$0.032^{j} \pm 0.011$
7	0.5	27.5	7.5	48	$0.181^{hi} \pm 0.006$
8	2	5	9	72	$0.415^{cde} \pm 0.112$
9	1.25	27.5	7.5	48	$0.692^{a} \pm 0.018$
10	0.5	50	9	72	$0.083^{ij} \pm 0.047$
11	0.5	50	9	24	$0.058^{j} \pm 0.004$
12	2	5	6	24	$0.201^{gh} \pm 0.017$
13	2	50	9	72	$0.447^{bcd} \pm 0.008$
14	1.25	27.5	7.5	48	$0.692^{a} \pm 0.028$
15	1.25	27.5	6	48	$0.312^{ef} \pm 0.046$
16	2	5	6	72	$0.342^{def} \pm 0.011$
17	1.25	27.5	7.5	48	$0.682^{a} \pm 0.011$
18	1.25	27.5	7.5	24	$0.471^{bc} \pm 0.049$
19	2	27.5	7.5	48	$0.534^{b} \pm 0.023$
20	1.25	50	7.5	48	$0.416^{cde} \pm 0.012$
21	0.5	5	9	24	$0.026^{j} \pm 0.010$
22	2	5	9	24	$0.427^{bcd} \pm 0.008$
23	2	50	6	72	$0.383^{cdef} \pm 0.097$
24	1.25	5	7.5	48	$0.304^{fg} \pm 0.033$
25	0.5	50	6	72	$0.075^{ij} \pm 0.008$
26	0.5	5	6	72	$0.019^{j} \pm 0.007$
27	2	50	9	24	$0.432^{bcd} \pm 0.011$
28	1.25	27.5	7.5	48	$0.682^{a} \pm 0.012$
29	2	50	6	24	$0.353^{def} \pm 0.009$
30	1.25	27.5	7.5	72	$0.701^{a} \pm 0.009$

Note: factor A: $AgNO_3$ concentration (mM) (min = 0.5, max = 2), factor B: ratio of $AgNO_3$/fungal filtrate (% v/v) (min = 5, max = 50), factor C: pH (min = 6, max = 9), factor D: synthesis period (hours) (min = 24, max = 72); the values in the table are the average of three replicates. In the same column, values followed by at least one letter are not significantly different at the 5% level of significance by Tukey's test.

Investigation of the antibacterial ability of the synthesized AgNPs

The experiment was carried out to investigate the antibacterial ability of AgNPs synthesized from the culture filtrate of fungus *T. virens* against Gram (−) pathogenic *E. coli* (ATCC® 25922TM), Gram (+) pathogenic *S. aureus* (ATCC® 25923TM), and *P. acnes* using the agar-well diffusion method.

Experimental design: The experiment employed a completely randomized design with the synthesized AgNPs at four dilution levels: 25%, 50%, 75%, and 100%. The positive control was 5 µg/mL streptomycin, and the negative control was the fungal filtrate. All the experiments were carried out in triplicate.

Conduct experiments: nano silver was diluted using distilled water to achieve a set of concentrations (25%, 50%, 75%, 100%). Bacterial strains were grown for 24 h in LB and TSB medium. The media for culturing *S. aureus*, *E. coli*, and *P. acnes* were prepared on petri dishes; the volume of medium for each dish was 15–20 mL. A volume of 50 µL of bacterial suspension (with a density of 10^7 CFU/mL, as determined by the counting method on agar plates) was spread onto the medium and dried for 15 min. Several wells were prepared by punching the agar medium (5 mm in diameter) into the petri dish to contain experimental treatments and controls. Then, 40 µL of AgNPs at four dilutions, a negative control, and 10 µL of a positive control were loaded into the wells. Each plate was incubated at 29°C for 24 h.

Evaluation criteria: the antibacterial activity was assessed by measuring the zone of inhibition at the 24-hour time point, calculated using the formula:

$$C = D - d \text{ (mm)}, \quad (1)$$

where: C – diameter of zone of inhibition; D – diameter of halo zone; d – well diameter.

Analyzing data

The data were processed using Excel software and Minitab 16 software to analyze variance and perform an ANOVA test, followed by a Tukey test at a 5% significance level.

Results and Discussion

Fungal isolation and identification

The isolated fungal samples were cultured on PDA me-

dium at 37 ± 2°C for 24 h, followed by observing the fungal growth, colony appearance, colony color, colony growth rate, colony morphology, conidial and phialide morphology, and size (Figure 1). As a result, the fungal mycelia were white, fast-growing, slightly spongy, and began to form conidia after culturing for 24 h. After 2 days of culture, the fungal mycelia became thick and spongy. The conidial color changed from white to varying shades of green. The flask body of the fungus was cylindrical and grew symmetrically to form clusters of 2–3 flasks on the top of the meristem sporangium. From the flask, conidia were formed. The conidia of the fungus are spherical or ovoid, with a smooth surface. The average size of conidia is about 2.9–3.1 x 2.3–3.3 µm. After 3 days of culture, the mycelium completely covered the plate and turned green on the fourth and fifth days (Figure 2).

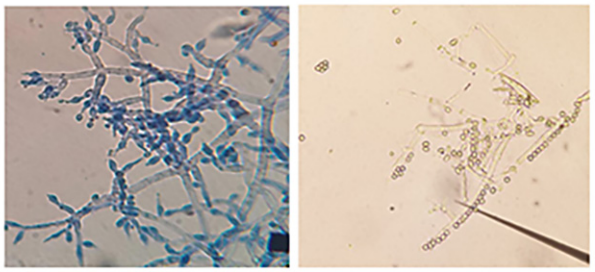

Fig. 1. Microscopic morphology (fungal mycelia, fungal conidia, and flask body) of the isolated fungi (Observed under the microscope under the magnification of X40 objective)

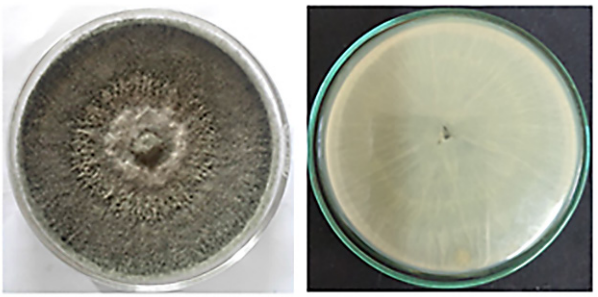

Fig. 2. Morphological characteristics of fungal isolates grown on PDA medium

Then, the preliminary identification of fungal species isolated from the collected soil samples typically resembled a strain of *Trichoderma* according to Rifai's (1969) taxonomic classification. Next, the sequencing technique based on the ITS gene region was used to determine the exact species name.

Results of identification using gene sequencing

To determine the precise species of *Trichoderma* sp., the internal transcribed spacer (ITS) sequencing was used. The electrophoresis results of the amplified rDNA–ITS region from the isolated *Trichoderma* fungus revealed a product band of approximately 500–600 bp in size (Figure 3).

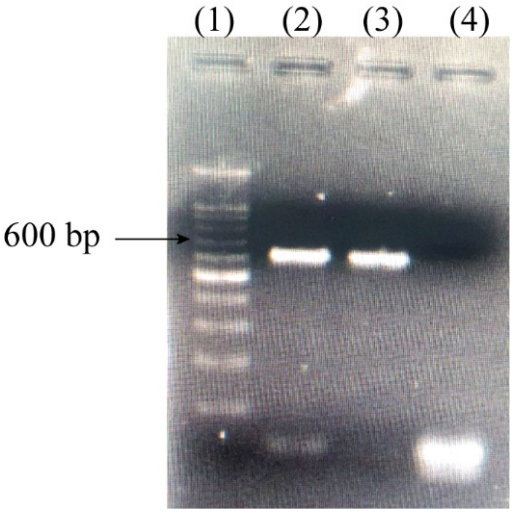

Fig. 3. Electrophoresis results of the amplified rDNA–ITS region of the isolated *Trichoderma* fungus (Note: well (1): standard ladder; well (2), (3): PCR product; well (4): negative control)

The results of gene sequencing showed that the sequence had good quality, clarity, and no interference, and the readable sequence was 500–550 nucleotides (nts). This sequence was searched and compared with homologous sequences on GenBank using NCBI's BLAST online software. The results of searching for homologous sequences showed that the sequences of the isolated *Trichoderma* resembled the ITS gene region of *T. virens*. The percentage of comparison fragments was 100% with sequence homogeneity of 99–100% with *T. virens* strain (Accession No. MN102106) (Figure 4).

Synthesis of AgNPs from fungal filtrate

The observation of the nano silver solution synthesized from the fungal filtrate and $AgNO_3$ after 24–72 h showed that the color gradually changed from a yellowish to a dark brown suspension (Figure 5). This result is consistent with previous studies by Shelar et al. (2015) and Saravanan et al. (2019) regarding the ability to form AgNPs from the filtrate of *Trichoderma* when reacting with an $AgNO_3$ solution. The color change of the solution can be explained by the excitation of surface plasmon vibrations of the AgNPs particles generated

select all 100 sequences selected GenBank Graphics Distance tree of results MSA Viewer

Description	Scientific Name	Max Score	Total Score	Query Cover	E value	Per. Ident	Acc. Len	Accession
Trichoderma virens isolate TrVi15 small subunit ribosomal RNA gene, partial sequence; internal transcribed spacer …	Trichoderma virens	935	935	100%	0.0	99.23%	617	PQ526690.1
Trichoderma virens isolate JUF0121 small subunit ribosomal RNA gene, partial sequence; internal transcribed spac…	Trichoderma virens	935	935	100%	0.0	99.23%	621	PX092196.1
Trichoderma sp. isolate TRICHO4 small subunit ribosomal RNA gene, partial sequence; internal transcribed spacer…	Trichoderma sp.	935	935	100%	0.0	99.23%	601	ON951823.1
Uncultured fungus isolate AS-24 small subunit ribosomal RNA gene, partial sequence; internal transcribed spacer 1…	uncultured fungus	935	935	100%	0.0	99.23%	637	PP125837.1
Trichoderma virens isolate B1 small subunit ribosomal RNA gene, partial sequence; internal transcribed spacer 1, 5…	Trichoderma virens	935	1051	100%	0.0	99.23%	682	PQ181534.1
Trichoderma virens strain GSR-2018-50A small subunit ribosomal RNA gene, partial sequence; internal transcribed…	Trichoderma virens	935	935	100%	0.0	99.23%	594	OM686860.1
Trichoderma sp. isolate 305_E9 small subunit ribosomal RNA gene, partial sequence; internal transcribed spacer 1…	Trichoderma sp.	935	935	100%	0.0	99.23%	622	PV348625.1
Trichoderma sp. isolate T1 small subunit ribosomal RNA gene, partial sequence; internal transcribed spacer 1, 5.8…	Trichoderma sp.	935	935	100%	0.0	99.23%	621	PP998531.1
Hypocrea sp. CRCF26 18S ribosomal RNA gene, partial sequence; internal transcribed spacer 1, 5.8S ribosomal R…	Trichoderma sp. …	935	935	100%	0.0	99.23%	576	HQ657314.1
Trichoderma virens isolate JUF0120 small subunit ribosomal RNA gene, partial sequence; internal transcribed spac…	Trichoderma virens	935	935	100%	0.0	99.23%	623	PX092195.1
Uncultured fungus clone seqFUN1-410 18S ribosomal RNA gene, partial sequence; internal transcribed spacer 1,…	uncultured fungus	935	935	100%	0.0	99.23%	639	KC191753.1
Trichoderma sp. isolate TRICHO15 small subunit ribosomal RNA gene, partial sequence; internal transcribed spac…	Trichoderma sp.	935	935	100%	0.0	99.23%	622	ON951834.1
Trichoderma sp. isolate PN8-1 internal transcribed spacer 1, partial sequence; 5.8S ribosomal RNA gene and inter…	Trichoderma sp.	935	935	100%	0.0	99.23%	600	PP437847.1
Trichoderma virens isolate 1036 internal transcribed spacer 1, partial sequence; 5.8S ribosomal RNA gene, comple…	Trichoderma virens	935	935	100%	0.0	99.23%	561	MG551576.1
Trichoderma virens isolate 201665E 18S ribosomal RNA gene, partial sequence; internal transcribed spacer 1, 5.8…	Trichoderma virens	935	935	100%	0.0	99.23%	600	MG650615.1
Trichoderma virens isolate A701 18S ribosomal RNA gene, partial sequence; internal transcribed spacer 1 and 5.8…	Trichoderma virens	935	935	100%	0.0	99.23%	579	KU529813.1
Trichoderma virens strain LW23 18S ribosomal RNA gene, partial sequence; internal transcribed spacer 1, 5.8S rib…	Trichoderma virens	935	935	100%	0.0	99.23%	620	KT803076.1
Uncultured fungus clone seqFUN1-205 18S ribosomal RNA gene, partial sequence; internal transcribed spacer 1,…	uncultured fungus	929	929	100%	0.0	99.04%	655	KC191748.1

Fig. 4. Results of comparison with data on Genbank NCBI by BLAST tool to search for sequences of similarity

by the reduction of Ag^{+} to Ag^{0}, catalyzed by enzymes that are secondary metabolites of *Trichoderma*. The control solution (without the $AgNO_3$ salt) showed no color change (Figure 5).

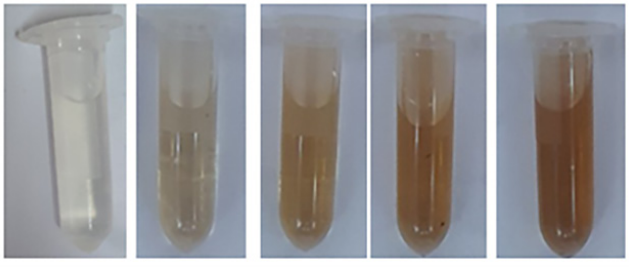

Fig. 5. Nano silver solution synthesized from fungal filtrate and $AgNO_3$ after 24–72 h of synthesis

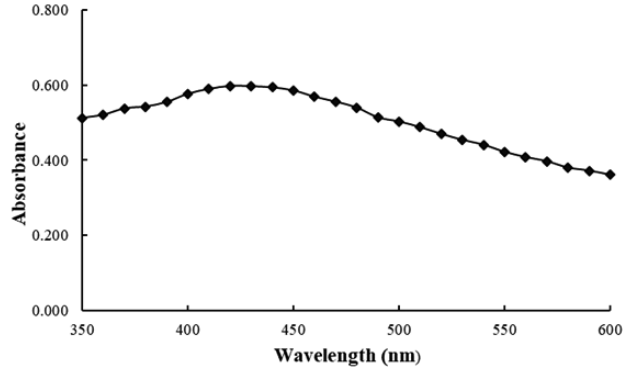

Fig. 6. Peak absorption spectra of the AgNPs sample formed in the wavelength range 350 nm – 600 nm

Figure 6 shows the results of the peak absorption spectroscopy analysis of the synthesized AgNPs in the wavelength range of 350–600 nm. The maximum absorption wavelength is in the range of 410–430 nm, with an absorbance of OD = 0.598.

Investigation of the influence of $AgNO_3$ concentration, ratio $AgNO_3$ solution/fungal filtrate (v/v), pH, and synthesis time on the formation of AgNPs

The resulting AgNPs have a uniform shape, small size, and uniform distribution. Table 2 illustrates the impact of the aforementioned four factors on AgNPs formation.

From the 30 treatments in Table 2, the data were uploaded to Design-Expert 13.0 software to evaluate the fit and significance of the model through analysis of ANOVA and the correlation index. The statistical results showed that the "P-value" was 0.0096 < 0.05, R^2 (R-Squared) was 0.9262, proving that the model was significant and acceptable. Besides, the statistical analysis of the expression of $AgNO_3$ concentration factor with a "P-value" of 0.0002 < 0.05 showed that $AgNO_3$

concentration influenced the OD measurement results at the wavelength of 420 nm with 99.99% confidence.

From the analytical values, the expected function value represented by the regression equation given by Design Expert 13.0 software is as follows:

$$OD = 0.6199 + 0.1655*A + 0.0297*B + 0.0464*C + \\ + 0.0249*D + 0.0024*AB + 0.0261*AC + \\ + 0.0081*AD - 0.0114*BC - 0.0039*BD \\ - 0.0094*CD - 0.1969*A^2 - 0.1944*B^2 \\ - 0.0574*C^2 + 0.0316*D^2 \quad (2)$$

The results showed that four combinations of $AgNO_3$ concentrations, the ratio of $AgNO_3$ solution to fungal filtrate, pH, and reaction time at treatments 17, 31, 56, and 69 gave the maximum absorbance value of the synthesized AgNPs at a wavelength of 420 nm. Selecting the conditions to optimize the nano silver synthesis reaction should be based on the optimization solutions given by the Design Expert 13.0 software in combination with equation (2). Therefore, to verify the correctness of the model, a control experiment was conducted to compare the four algorithm model optimization treatments presented in Table 3 and the comparison chart in Figure 7.

Treatment 56 yielded the highest actual OD420 nm value, demonstrating that the optimal conditions for AgNPs synthesized from fungal filtrate were: an $AgNO_3$ concentration of 1.6 mM, a $V_{AgNO3}/V_{fungal\ filtrate}$ ratio of 27.4%, a pH of 7.9, and a reaction time of 71.2 h.

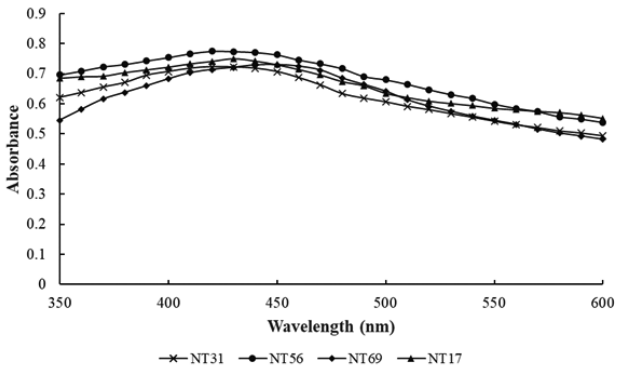

Fig. 7. Maximum absorption spectra of AgNPs samples formed in four optimal treatments in the wavelength range 350 nm–600 nm

The SEM image of AgNPs synthesized from the fungal filtrate showed that AgNPs have a spherical shape and are not uniform in size. The particles have a large size, ranging from 70 nm to 100 nm in diameter (Figure 8). The large size of AgNPs can be attributed to an extended reaction time due to the transportation of samples for SEM measurement.

Some studies show a relationship between the shape and size of AgNPs and their antibacterial ability; smaller AgNPs yield higher antibacterial activity than larger particles. Smaller sizes with a large total specific surface area can be more effective in killing bacteria (Choi et al., 2008; Li et al., 2009).

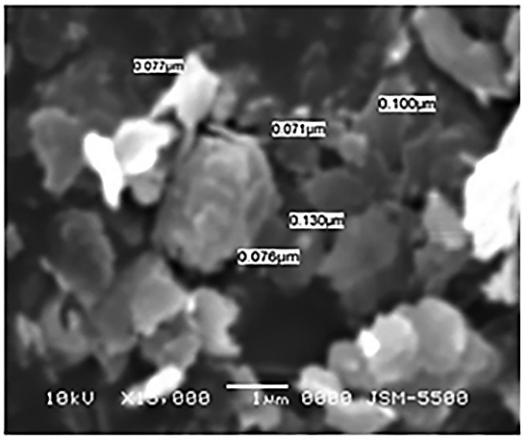

Fig. 8. AgNPs under scanning electron microscope (SEM)

Antibacterial results of AgNPs by agar well diffusion method

Antibacterial ability of synthesized AgNPs against *S. aureus*: The negative control, which was fungal filtrate without AgNPs, exhibited no zone of inhibition. It can be concluded that the antibacterial activity against *S. aureus* is due to the role of the synthesized AgNPs (Figure 9 and Table 4).

Table 3. The results of OD 420 nm for 4 optimal treatments

Treatment	[$AgNO_3$]	Ratio	pH	Reaction times	Expected OD	Measured OD
56	1.6	27.4	7.9	71.2	0.721	$0.775^a \pm 0.008$
17	1.6	29.4	8.3	70.1	0.718	$0.738^b \pm 0.015$
69	1.5	26.1	7.9	71.7	0.716	$0.714^b \pm 0.018$
31	1.5	30.3	8.2	71.8	0.716	$0.723^b \pm 0.015$

Note: the values in the table are the average of three replicates. In the same column, values, followed by at least one letter are not significantly different at the 5% level of significance by Tukey's test.

Table 4. Inhibition of AgNPs synthesized from fungal filtrate against *S. aureus*

AgNPs concentration	Zone of inhibition, mm
Positive control (+)	$16.07^{a} \pm 0.22$
100%	$8.83^{b} \pm 0.18$
75%	$6.70^{c} \pm 0.13$
50%	$4.80^{d} \pm 0.33$
25%	$3.37^{e} \pm 0.22$

Note: The diameter zone of inhibition is the average value of three replicates. In the same column, mean values followed by at least one letter are not significantly different at 5% level by Tukey test. The negative control has not performed inhibitory zone

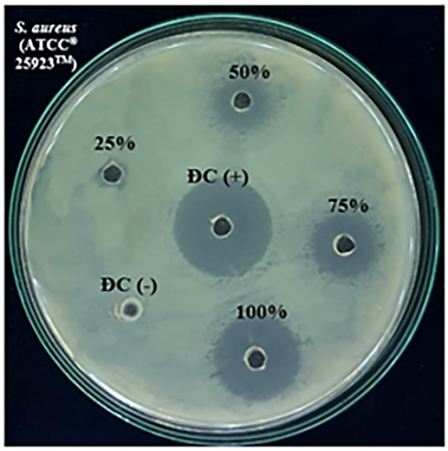

Fig. 9. Antimicrobial activity of *T. virens* mediated AgNPs against *S. aureus.*
(ĐC (-): negative control; ĐC (+): positive control; 25 %, 50 %, 75 %, 100 %: treatments)

Table 4 shows the antimicrobial activity of nano silver synthesized from fungal filtrate, which was recorded after incubating for 24 h. The results showed that as the concentration increased, the value of the ZOI also increased, with the ZOI rising by approximately 2 mm when the AgNP concentration increased by 25%. Nano silver at 100% concentration exhibited the highest inhibition against *S. aureus,* with a ZOI value of 8.83 ± 0.18 mm. In the two treatments, the ZOI of the 50% and 75% dilution concentrations were 4.80 ± 0.33 mm and 6.70 ± 0.13 mm, respectively. Meanwhile, nano silver at 100% concentration exhibited the lowest inhibition, with a ZOI of 3.37 ± 0.22 mm. The comparison results of all four AgNPs concentrations were statistically significantly different from the control treatment.

Antibacterial ability of the synthesized AgNPs against E. coli

After 24 h of investigation, all concentrations of nano silver showed the ability to inhibit the growth of *E. coli*. Figure 10 illustrates that the diameter of ZOI increases gradually with increasing AgNP concentrations. Meanwhile, in the negative control treatment, no inhibited zone formation was observed. The experiment demonstrated that the synthesized nano silver has an antibacterial effect against *E. coli*.

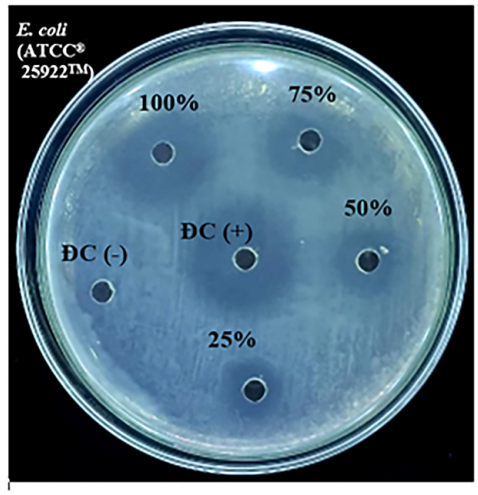

Fig. 10. Antimicrobial activity of *T. virens* mediated AgNPs against *E. coli.*
(ĐC (-): negative control; ĐC (+): positive control; 25 %, 50 %, 75 %, 100 %: treatments)

In general, all three concentrations of nano silver showed the ability to inhibit *E. coli*. Table 5 shows that a higher concentration of AgNPs has a greater inhibitory ability. The ZOI increased by approximately 2.5 mm when the concentration of AgNPs was increased by 25%. The highest ZOI value was obtained when the 100% concentration of AgNPs was used. The inhibited zone was 11.93 ± 0.24 mm in diameter. The ZOI values at concentrations of 50% and 25% did not show

Table 5. Inhibition of AgNPs synthesized from fungal filtrate against *E. coli*

AgNPs concentration	Zone of inhibition, mm
Positive control (+)	$17.33^{a} \pm 0.58$
100%	$11.93^{b} \pm 0.24$
75%	$8.07^{c} \pm 0.18$
50%	$6.33^{d} \pm 0.42$
25%	$5.30^{d} \pm 0.33$

Note: The diameter zone of inhibition is the average value of three replicates. In the same column, mean values followed by at least one letter are not significantly different at 5% level by Tukey test. The negative control has not performed inhibitory zone

statistically significant differences at a 5% significance level. Nano silver at a concentration of 25% yielded the lowest inhibitory effect, with a ZOI of 5.30 ± 0.33 mm.

From the results in Table 5, it is evident that AgNPs synthesized from fungal filtrate at a 100% concentration exhibit a good inhibitory effect on *E. coli*. The ability of AgNPs to adhere to the surface of the cell membrane and affect the osmotic activity of the cell endows AgNPs with strong antibacterial ability. The AgNPs not only interact with the surface of the membrane but also penetrate bacteria, destroying bacterial cells by interacting with the sulfate and phosphorus functional groups present in DNA and proteins, thereby altering their structure and function (Sangaonkar and Pawar, 2018).

Antibacterial ability of the synthesized AgNPs against P. acnes

When the concentration of nano silver increased, the antimicrobial effect also increased. The negative control did not form an inhibited zone, demonstrating that AgNPs have an antibacterial effect against *P. acnes* (Figure 11).

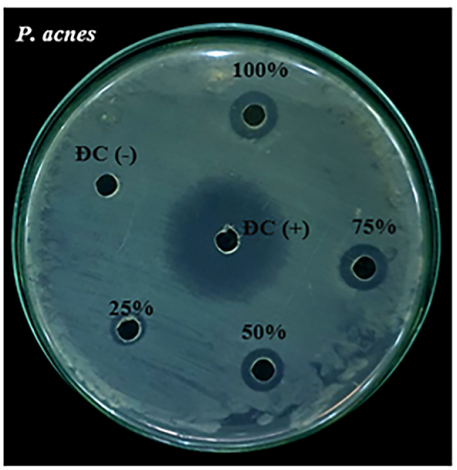

Fig. 11. Antimicrobial activity of *T. virens* mediated AgNPs against *P. acnes.*
(ĐC (-): negative control; ĐC (+): positive control; 25 %, 50 %, 75 %, 100 %: treatments)

From Table 6, it can be seen that when the concentration of AgNPs increases by 25%, the diameters of the bacterial inhibition zones also increase by about 2 mm. For the concentration of nano silver at 100%, the highest resistance against *P. acnes* was 6.67 ± 0.29 mm. The ZOI value was 4.73 ± 0.58 mm when the silver concentration was 75%. The concentrations between 25% and 50% showed that the difference was not statistically significant at the 5% level of significance. The lowest resistance to *P. Acnes* was at 25% with a ZOI of 1.50 ± 0.20 mm.

Table 6. Control values of nano-silver concentrations synthesized from fungal filtrate against *P. acnes*

AgNPs concentration	Zone of inhibition, mm
Positive control (+)	$16.77^{a} \pm 0.42$
100%	$6.67^{b} \pm 0.29$
75%	$4.73^{c} \pm 0.58$
50%	$2.80^{d} \pm 0.20$
25%	$1.50^{d} \pm 0.20$

Note: The diameter zone of inhibition is the average value of three replicates. In the same column, mean values followed by at least one letter are not significantly different at 5% level by Tukey test. The negative control has not performed inhibitory zone.

Through investigation of the resistance of synthesis AgNPs from fungal filtrate in three types of bacteria – *E. coli*, *P. acnes*, and *S. aureus*, it can be seen that AgNPs have the highest antimicrobial activity against *E. coli* and the lowest antimicrobial activity against *P. acnes*. The gram-positive bacteria showed a smaller zone of inhibition, while the gram-negative bacteria showed a larger zone of inhibition. The presence of a peptidoglycan layer in Gram-positive bacteria may be a reason for reduced activity, as it can prevent nanoscale particles from entering the cell wall (Shrivastava et al., 2007). The higher antibacterial activity was undoubtedly due to the AgNPs, as the negatively charged bacterial cells were more attracted towards silver ions, causing bacterial cell wall rupture. Lok et al. (2006) demonstrated that bacterial cell membranes and plasma membranes were destabilized by AgNPs, resulting in the depletion of intracellular ATP. Silver ions and silver-based compounds showed vigorous antimicrobial activity. They have a large surface area with strong reactive sites. Earlier, it was demonstrated that the antibacterial activity of AgNPs is size- and shape-dependent. Silver nanoscale particles (1–10 nm) attach to the surface of the cell membrane and drastically disrupt its functions, such as respiration and permeability (Morones et al., 2005). This can also be explained by the fact that *P. acnes* can create biofilms. Biofilm production is considered a mechanism that helps some microorganisms, including *P. acnes,* to survive when the environment becomes unfavorable for their growth. Bacterial biofilms are constructed to enclose bacterial cells within an extracellular polymer matrix, a polymeric combination of DNA, proteins, and polysaccharides (Ramage et al., 2003). The ability to create biofilms of *P. acnes* explains why the inhibitory effect of nano silver is lower than that of *E. coli* and *S. aureus*.

Several previous studies have demonstrated that exposing nano silver to bacterial cells can interact with the thiol functional group in cellular enzymes, generating free radicals. This leads to changes in the respiratory chain within the cell membrane and can result in bacterial cell death (Shahzadi et al, 2014).

Conclusions

Nano silver was synthesized from fungal filtrate with the optimized conditions: $AgNO_3$ concentration at 1.6 mM, ratio of $V_{AgNO3}/V_{fungal\ filtrate}$ at 27.4%, the synthesized medium with pH = 7.9, and the reaction time around 71.2 h. SEM images indicate that the AgNPs have a spherical shape with sizes ranging from 70 to 100 nm. Nano silver also demonstrated antibacterial effectiveness against three bacteria, *E. coli*, *P. acnes*, and *S. aureus,* at four concentrations: 25%, 50%, 75%, and 100%. The higher the concentration, the stronger the antibacterial ability. The 100% concentration yielded the strongest antibacterial effect against *E. coli*, *S. aureus*, and *P. acnes,* with the diameter of the inhibited zone being approximately 11.93 ± 0.24 mm, 8.83 ± 0.18 mm, and 6.67 ± 0.29 mm, respectively. In addition, nano silver has higher resistance to *E. coli* as compared to the other two bacteria.

References

Berdy, J. (2005). Bioactive microbial metabolites. A personal view. *The J. Antibiot., 58*(1), 1 – 26.

Bui, L., Huynh, P., Luu, M. C. & Nguyen, N. T. (2021). Optimization of the lactic acid fermentation from tofu sour liquid and application in the production of antibacterial soap against *Propionibacterium acnes PO. TNU Journal of Science and Technology, 226*(10), 9 – 17.

Choi, O., Deng, K. K., Kim, N. J., Ross, L. Jr., Surampalli, R. Y. & Hu, Z. (2008). The inhibitory effects of silver nanoparticles, silver ions, and silver chloride colloids on microbial growth. *Water Res., 42*(12), 3066 – 3074. doi: 10.1016/j.watres.2008.02.021.

Elad, Y., Chet, I. & Henis, Y. (1982). Degradation of plant pathogenic fungi by *Trichoderma harzianum*. *Can. J. Microbiol., 28*(7), 719 – 725. doi: 10.1139/m82-110.

Li, W., Raoult, D. & Fournier, P-E. (2009). Bacterial strain typing in the genomic era. *FEMS Microbiol. Rev.*, *33*(5), 892 – 916.

Lok, C. N., Ho, C. M., Chen, R., He, Q. Y., Yu, W. Y., Sun, H., Tam, P. K., Chiu, J. F. & Che, C. M. (2006). Proteomic analysis of the mode of antibacterial action of silver nanoparticles. *J. Proteome Res., 5*(4), 916 – 924.

Loo, Y. Y., Rukayadil, Y., Nor−Khaizura, M. A. R., Kuan, C. H., Chieng, B. W., Nishibuchi M. & Radu, S. (2018). *In vitro* antimicrobial activity of green synthesized silver nanoparticles against selected gram-negative foodborne pathogens. *Front. Microbiol.*, *9*, 1555.

Morones, J. R., Elechiguerra, J. L., Camacho, A., Holt, K., Kouri, J. B., Ramírez, J. T. & Yacaman, M. J. (2005). The bactericidal effect of silver nanoparticles. *Nanotechnology, 16*(10), 2346 – 2353.

Ramage, G., Tunney, M. M., Patrick, S., Gorman, S. P. & Nixon, J. R. (2003). Formation of *Propionibacterium acnes* biofilms on orthopaedic biomaterials and their susceptibility to antimicrobials. *Biomaterials, 24*(19), 3221 – 3227.

Rifai, M. A. (1969) A revision of the genus *Trichoderma. Mycol. Pap., 116*, 1 – 56.

Saravanan, K., Anitha, M., Rajabairavi, N., Arivazhagan, P. & Jayakumar, S. (2019). Biosynthesis of silver nanoparticles from Trichoderma Harzianum and its impact on germination status of rice and brinjal. *Int. J. Pharma Bio Sci., 9*(1), 157 – 162.

Shelar, G. B. & Chavan, A. M. (2015). Myco-synthesis of silver nanoparticles from *Trichoderma harzianum* and its impact on germination status of oil seed. *Biolife, 3*(1), 109 – 113.

Shrivastava, S., Bera, T., Roy, A., Singh, G., Ramachandrarao, P. & Dash, D. (2007). Characterization of enhanced antibacterial effects of novel silver nanoparticles. *Nanotechnology, 18*(22), 22510.

Wang, X. J., Hayes, J. D., Henderson, C. J. & Wolf, C. R. (2007). Identification of retinoic acid as an inhibitor of transcription factor Nrf2 through activation of retinoic acid receptor alpha. *PNAS USA, 104*(49), 19589 – 19594.

Sangaonkar, G. M. & Pawar, K. D. (2018). Garcinia indica mediated biogenic synthesis of silver nanoparticles with antibacterial and antioxidant activities. *Colloids and surfaces. B, Biointerfaces*, *164*, 210 – 217.

Shahzadi, S., Fatima, S., Ul Ain, Q., Shafiq, Z. & Janjua, M. R. S. A. (2025). A review on green synthesis of silver nanoparticles (SNPs) using plant extracts: a multifaceted approach in photocatalysis, environmental remediation, and biomedicine. *RSC advances, 15*(5), 3858 – 3903.

Received: **April, 13, 2024**; *Approved*: **May, 23, 2024;** *Published:* **October, 2025**